Immunity 25, 963–975, December 2006 ©2006 Elsevier Inc. DOI 10.1016/j.immuni.2006.10.015

Tracing Hematopoietic Precursor Migration to Successive Hematopoietic Organs during Zebrafish Development

Emi Murayama,[1,4] Karima Kissa,[1,4] Agustin Zapata,[2] Elodie Mordelet,[1] Valérie Briolat,[1] Hui-Feng Lin,[3] Robert I. Handin,[3] and Philippe Herbomel[1,*]

[1] Unité Macrophages et Développement de l'Immunité
CNRS-URA 2578
Institut Pasteur
25 rue du Dr Roux
75724 Paris cedex 15
France

[2] Department of Cell Biology
Faculty of Biology
Complutense University
28040 Madrid
Spain

[3] Hematology Division
Brigham and Women's Hospital
1 Blackfan Circle
Boston, Massachusetts 02115

Summary

Although the ontogeny of hematopoietic stem cells (HSCs) in vertebrates has been studied intensely, a lineage relationship between the HSCs found in the developmentally successive hematopoietic organs remains to be shown. By using an in situ photoactivatable cell tracer in the transparent zebrafish embryo, we demonstrated that definitive blood precursors appeared between the dorsal aorta and axial vein, validating the homology of this tissue with the AGM (aorta-gonad-mesonephros) of amniotes. These cells first migrated through the blood to a previously undescribed caudal hematopoietic tissue (CHT), where they differentiated, expanded, and further migrated to seed the definitive hematopoietic organs, the thymus and kidney. Immigrants on the way to the thymus expressed *c-myb* and *ikaros* but not *rag1*; they were probably no longer HSCs, however, because they lacked *scl* and *runx1* expression, unlike immigrants to the kidney. The CHT thus has a hematopoietic function similar to that of the mammalian fetal liver.

Introduction

In the ontogeny of vertebrates, hematopoiesis occurs in several successive organs. The first or "primitive" hematopoiesis provides the embryo with erythrocytes and macrophages, both of which differentiate quickly from mesoderm, in the yolk sac for most vertebrate species. The later hematopoietic sites give rise to more diverse progeny, including lymphoid cells. In the adult, the continuous production of all blood cell lineages relies on the existence of hematopoietic stem cells (HSCs). HSCs, i.e., cells with long-term multilineage reconstitution potential, are also found in the fetal hematopoietic organ, the liver in mammals, and in the latter their number is known to expand greatly. A decade ago, it was discovered that the first site in ontogeny where HSCs can be detected, the so-called AGM (aorta-gonad-mesonephros) area, is distinct from those where multilineage hematopoietic differentiation will take place (Godin and Cumano, 2002). This and other data led to the assumption that the HSCs generated in the AGM migrate to give rise to the HSCs and all hematopoietic cells later found in the liver and then in the bone marrow. Yet such a lineage relationship remains to be directly shown.

The zebrafish embryo, owing to its accessibility and transparency and the recent development of molecular tools and transgenic fluorescent reporter lines, is especially suitable to study in vivo the successive stages in the establishment of definitive hematopoiesis and the cell migrations involved. However, so far, only primitive hematopoiesis, which takes place within the first 24 hr postfertilization (hpf), has been studied substantially in zebrafish. Very little is known about the establishment of definitive hematopoiesis (Davidson and Zon, 2004). By 26 hpf, as the primitive blood cells have just started circulating, genes involved in specifying definitive HSCs from mesoderm in mammals, *c-myb* and *runx1*, start to be expressed in a cell cord all along the trunk, just ventral to the dorsal aorta (DA). The analogy of this location with that of the AGM in mammals led to the suggestion that these cells might be the definitive HSCs (Thompson et al., 1998). Recently it was shown that suppressing *runx1* expression or Notch signaling causes suppression of both *c-myb* expression ventral to the DA at 26 hpf and *rag1* expression in the thymus 4 days later (Gering and Patient, 2005; Burns et al., 2005). This observation suggests but does not prove a lineage link between the two cell populations. Up to now, there has been no functional characterization or cell-tracing study of these presumed HSC progenitors from the trunk. Possible sites of larval hematopoiesis, analogous to the mammalian liver, have not been investigated either.

In adult teleost fishes, hematopoiesis occurs in the kidney, in the vestiges of the pronephros and between the tubules of the mesonephros, the definitive kidney. In zebrafish, the kidney starts producing mature myeloid and lymphoid cells by 2 weeks of development (Willett et al., 1999). And yet, the thymus starts being colonized by lymphoblasts by 3 days pf (dpf; Willett et al., 1999), and neutrophilic granulocytes (Willett et al., 1999; Lieschke et al., 2001) as well as prothrombocytes (Lin et al., 2005) can be found in the embryo by 2 dpf—suggesting the existence of an intermediate (larval) site of hematopoiesis, after the primitive wave and before the kidney starts producing all leukocyte cell types.

The present work shows that larval hematopoiesis takes place in the ventral tail, initiated around a transient structure, the caudal vein plexus. By using a photoactivatable cell tracer, we establish that hematopoietic precursors present in the presumptive zebrafish AGM migrate through the blood to seed the stroma of the tail. There they differentiate, and also expand, mature,

*Correspondence: herbomel@pasteur.fr

[4] These authors contributed equally to this work.

and migrate to seed the definitive hematopoietic organs, the thymus and kidney, these two destinations correlating with distinct precursor phenotypes.

Results

In Vivo Identification of a New Site of Hematopoiesis in the Ventral Tail

In our video-enhanced DIC (differential interference contrast) microscopic observations of live zebrafish embryos during their first week of development (Herbomel et al., 1999, 2001), we noticed the presence in the ventral part of the tail, in the mesenchyme around the caudal vein (CV) plexus (Figure 1A), of increasing numbers of round cells with the morphology of hematopoietic precursors or lymphocytes (scant cytoplasm and a round nucleus with condensed clumps of chromatin), with cell sizes ranging from 5.5 to 10.5 μm (Figures 1B–1F, see Movies S1–S4 in the Supplemental Data available online). These cells appeared more likely to be hematopoietic precursors than lymphocytes, because no lymphocyte marker is expressed in zebrafish embryos and early larvae except in the nascent thymus (Langenau et al., 2004). Mitoses were frequently observed among these various presumptive precursors (Figure S1). In CD41-gfp and gata1-dsred transgenic embryos (Traver et al., 2003; Lin et al., 2005), a substantial fraction of these cells expressed green fluorescent protein (GFP) or DsRed fluorescent protein at levels detectable by fluorescence microscopy (Figures 1G and 1H, and Figures S2C and S2C′; data not shown). Between them, we also identified macrophages, which displayed increasing amounts of phagocytosed material with time (Figure 1E, arrows), and granulocytes recognizable by DIC through their constantly moving, refringent cytoplasmic granules (Movie S3).

The expansion of this hematopoietic population paralleled the development of the CV plexus and its further evolution into a single caudal vein. When blood circulation started, by 25 hpf, the initial CV was a single-channel vessel in close apposition to the caudal artery (CA), but already sprouting along its entire length in ventral direction (Figure S2A, arrows). The growing venous segments soon anastomosed and transformed the single-channel CV into a branched plexus, throughout which the blood flowed by 35 hpf (Movie S1, Figure S2B; Figure 1G; see also Isogai et al., 2001). Hematopoietic precursors could soon be observed around the dorsal part of this venous plexus (Figure 1B), between the caudal artery and the ventral limit of the flanking somitic muscles. Caudal hematopoiesis thereafter remained confined between these two boundaries. This could be visualized with CD41-gfp and gata1-dsred double transgenic embryos (Figures 1G and 1H). The CV plexus, which by 48 hpf extended largely beyond the ventral limit of the somitic muscles, became entirely covered by them on either side within the next 24 hr (Figures 1G and 1H and Figures S2G–S2I). Morphometric measurements revealed that this was not due to a dorsoventral growth of the somitic muscles, but to a retraction of the CV plexus back to within the medial space between the somites, leaving only its ventral-most channel, the future definitive CV, outside, in contact with the somitic muscles (Figure 1H and Figures S2G–S2I).

In parallel, the blood had progressively ceased flowing through most of the CV plexus but the definitive CV (Isogai et al., 2001). Yet the fli-gfp transgenic line (Lawson and Weinstein, 2002), in which all vascular cells express the GFP, revealed that the vascular elements of the CV plexus were still present until 5 dpf, while the hematopoietic cell content of the tissue was increasing (Figure S2C). Some of these elements were rewired to connect the intersomitic veins to the definitive CV, and the remaining ones progressively merged with the latter (Figure 1H and Figures S2D–S2F).

As hematopoietic precursors accumulated around the CV plexus, increasing numbers appeared marginated in the lumen of the definitive CV, as single cells or small clusters of cells by 3 dpf, and then as larger groups by 5–7 dpf (Figure 1E). A presumptive hematopoietic progenitor was observed in the CV rolling over one such intravenous cluster of another (larger) kind of progenitors (Movie S4).

By 3 dpf, the caudal hematopoietic tissue had extended into the adjacent trunk, typically up to 2–3 somites rostral to the cloaca; by 4 dpf, discontinuous, smaller patches of hematopoietic progenitors occurred even more rostrally (data not shown). Between 2.5 and 4 dpf, the initially coalescent DA and posterior cardinal vein (PCV, Figure 1A) had been moving apart from each other, leaving an interstitial space in between, where these colonies occurred, in contact with the PCV, mostly at intersomitic boundaries. After 6 dpf, the size of the caudal hematopoietic cell clusters decreased, first in the mesenchymal space, then also in the CV lumen. However, hematopoietic progenitors were still present there at 10 and 14 dpf (see below). Thus, the transient CV plexus and its subsequent remnants appear to constitute a niche for the expansion of hematopoietic progenitors in the developing zebrafish larva.

Early Hematopoietic Markers Reveal the Transition of Hematopoiesis from the Tail to the Kidney

The expression of early hematopoietic markers in zebrafish has rarely been examined past 48 hpf. Liao et al. (1998) found that by 4 dpf, *scl* and *c-myb* were most strongly expressed in the ventral tail area, but that their expression there subsided by 5 dpf. We examined this in more detail in the light of our in vivo observations and extended the analysis to two other early acting hematopoietic transcription factors, *runx1* and *ikaros* (Figure 2; Gering and Patient, 2005).

At 26 and 35 hpf, *c-myb* was expressed all along the trunk in a cell cord between the closely joined DA and PCV (DA-PCV joint), from somite 6 to the cloaca (somite 17/18) (Figures 2A and 2B). Progressively, this *c-myb*$^+$ cell cord extended more into the tail. At 48 hpf, in some embryos, expression is already higher there than in the trunk, lighting up cell clusters that abut the CA dorsally and the somite muscle limit ventrally (Figure S3A, arrows), consistent with our in vivo observations. At 3 dpf, *c-myb* expression was still detected in the trunk, but had become higher in the ventral tail between CA and CV (data not shown). *c-myb* was also expressed in the branchial arches (Figure 2C, green arrows) and in the nascent thymus (Figure S3C). At 4 dpf, c-myb-positive cells were detected for the first time in the pronephros around the glomerulus (Figure 2E) and in the heart

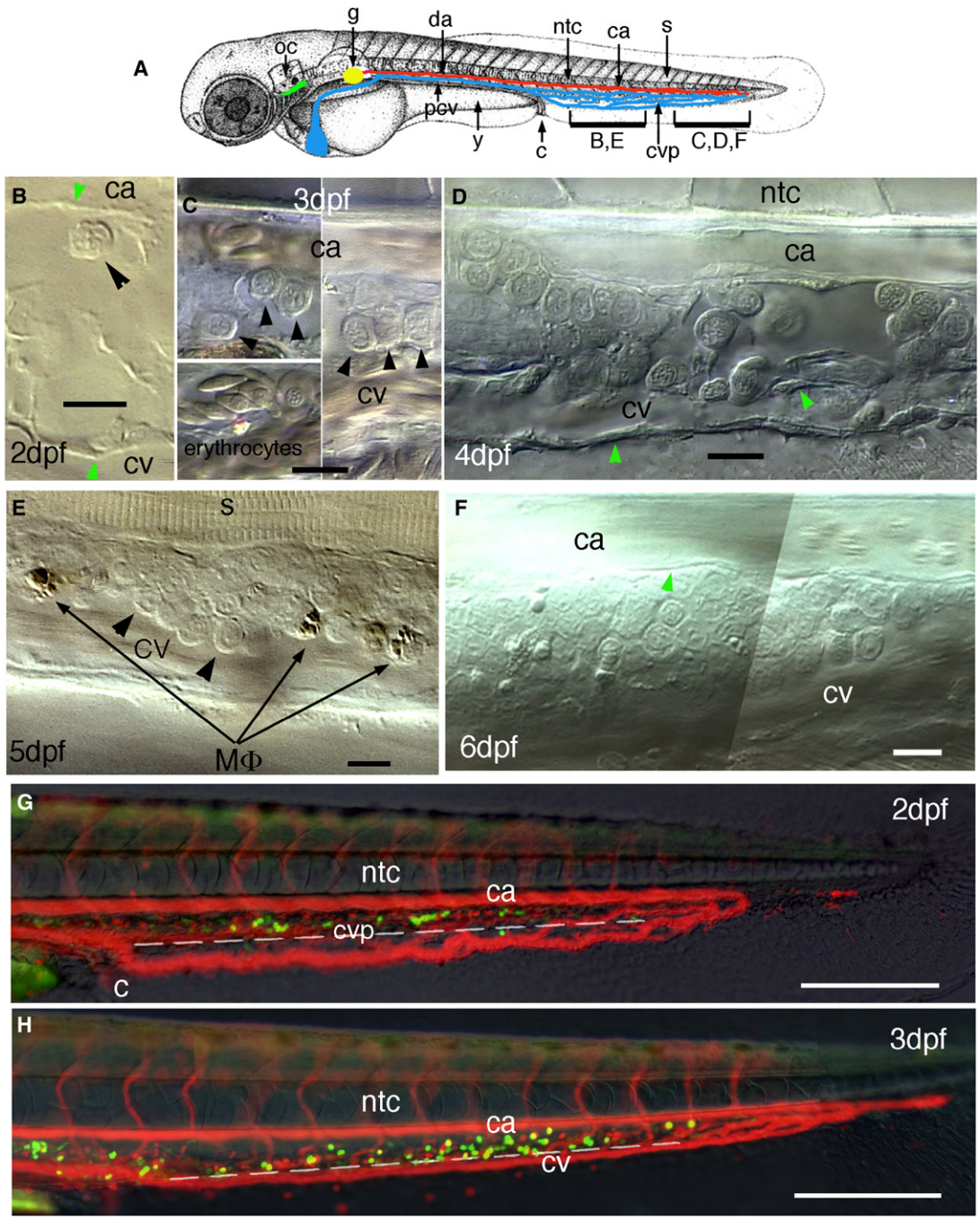

Figure 1. In Vivo Observation of Hematopoietic Progenitors in the Ventral Tail of Zebrafish through the First Week of Development

(A) Anatomical landmarks used in this study: dorsal aorta (da), posterior cardinal vein (pcv), cloaca (c), caudal artery (ca), caudal vein plexus (cvp), thymus (green), pronephric glomerulus (g, yellow), notochord (ntc), somite muscles (s), otic capsule (oc).

(B–F) Video-enhanced DIC microscopic observation in the ventral tail, showing progressive accumulation of hematopoietic progenitors (a few shown by black arrowheads) between the CA and definitive CV; (B) 2 dpf; (C) 3 dpf; the lower left panel shows for comparison, both in flat and profile view, the distinct shape of primitive erythrocytes past 2.5 dpf, with a very small nucleus (3.5 μm) and flat elliptical cytoplasm; (D) 4 dpf; (E) 5 dpf; (F) 6 dpf. Green arrowheads, vascular endothelium; MΦ, macrophages.

(G and H) DIC, red and green fluorescence overlay images of a gata1-dsred, CD41-gfp double transgenic embryo at (G) 2 dpf and (H) 3 dpf; a dotted line indicates the ventral limit of somite muscles; circulating DsRed^{+} primitive erythrocytes delineate the blood flow.

All lateral views, rostral to the left. Scale bars represent 10 μm in (B)–(F), 100 μm in (G) and (H).

chambers (data not shown). At 5–6 dpf, *c-myb* expression in the tail reached its highest level; c-myb^{+} cells were arranged all along and dorsal to the CV and tended to be more numerous between successive somites, where more space is available because of somite curvature (Figure 2C). They formed strings separated by or sometimes encircling clusters of c-myb-negative cells (Figure 2I, purple arrows). In the trunk, by 4 dpf the DA

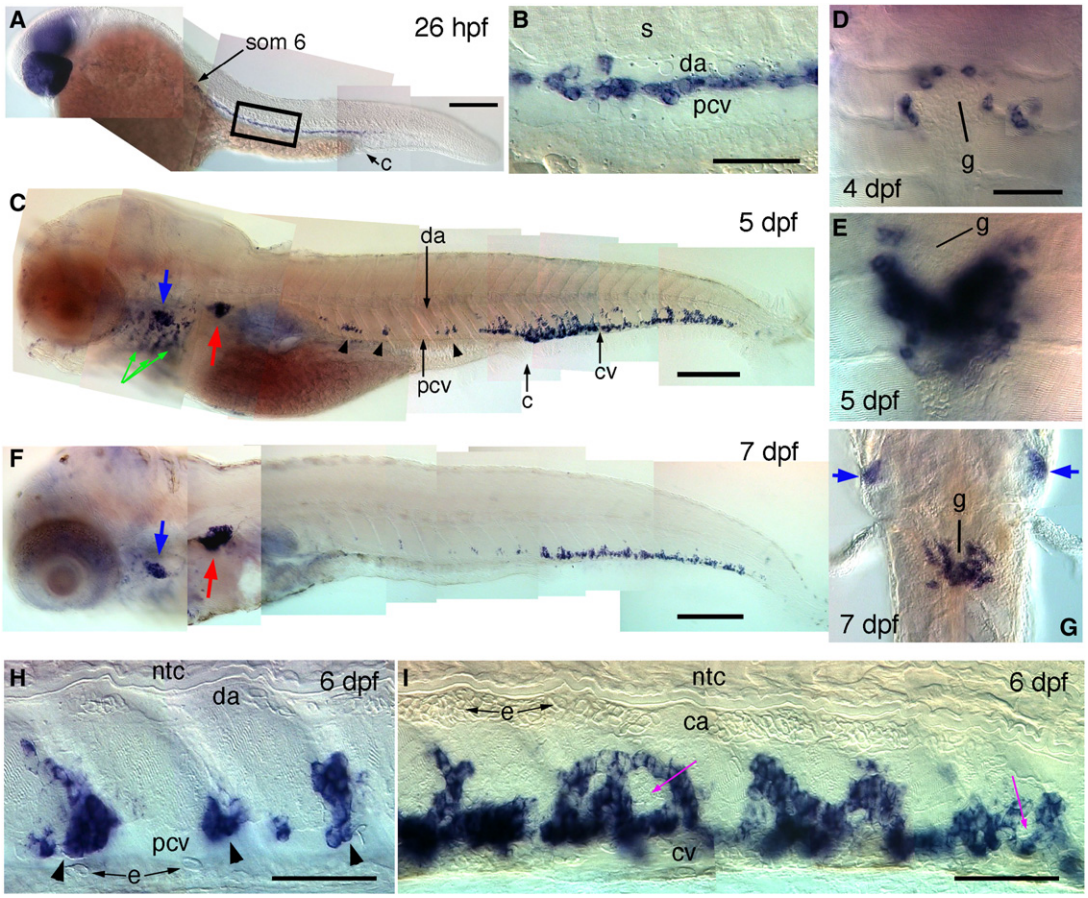

Figure 2. *c-myb* Expression Reveals the Successive Sites of Larval and Definitive Hematopoiesis

Whole-mount in situ hybridization at successive developmental stages.

(A) 26 hpf, short after blood circulation onset; position of somite 6 is indicated.

(B) Close-up on the area boxed in (A).

(C) 5 dpf.

(D and E) Ventral views (rostral up) of c-myb$^+$ cells around the pronephric glomerulus (g) at (D) 4 dpf and (E) 5 dpf.

(F) 7 dpf.

(G) Ventral view (rostral up) of the pronephric region at 7 dpf.

(H and I) Higher magnification lateral views (rostral left) of c-myb$^+$ cells in (H) the trunk and (I) the tail, occurring around c-myb$^-$ cell clusters (purple arrows).

e, primitive erythrocytes; blue arrows, thymus; red arrows, pronephros; green arrows, branchial arches; arrowheads, c-myb$^+$ patches along the PCV. Scale bars represent 200 μm in (A), (C), and (F); 50 μm otherwise.

and PCV had moved apart from each other, and from then onward, sporadic c-myb$^+$ cell colonies occurred, mainly in the intersomitic spaces, dorsal to and in contact with the PCV (Figures 2C and 2H, arrowheads).

More rostrally, *c-myb*$^+$ cells were now numerous in the thymus (Figures 2C, 2F, 2G, blue arrows) as well as around the pronephric glomerulus (Figure 2C, red arrow, and Figure 2E). At 7 dpf, *c-myb* expression had decreased in the ventral tail, but was still increasing in the pronephros, which now was its major site of expression (Figures 2F and 2G).

The hematopoietic expression of *scl* was scarce from 26 to 48 hpf. Only weak *scl* expression could be detected in some cells of the DA-PCV joint where *c-myb* and *runx1* expression was found (data not shown). In contrast, from 3 to 7 dpf, *scl* was strongly expressed first in the tail (and smaller colonies along the PCV in the trunk) and then in the kidney, in a space-time pattern indistinguishable from that of *c-myb* (Figures S3D–S3F). Unlike *c-myb, scl* was not expressed in the nascent thymus.

The hematopoietic expression of *runx1* up to 7 dpf was identical to that of *c-myb* both in location and time course—except that like *scl*, *runx1* was not expressed in the thymus (Figure S3H, and data not shown). Finally, *ikaros* was first expressed in the trunk DA-PCV joint several hours later than *runx1* and *c-myb* (data not shown), and then its hematopoietic expression pattern closely followed that of *c-myb*, in the tail, thymus, and kidney (Figures S3B, S3G, and S3I).

Thus, the expression analysis of all four early hematopoietic markers support the hypothesis that the mesenchyme around the caudal vein plexus is the first and main site of larval hematopoiesis during the first week of zebrafish development, after which the pronephros becomes the main and definitive site of hematopoiesis.

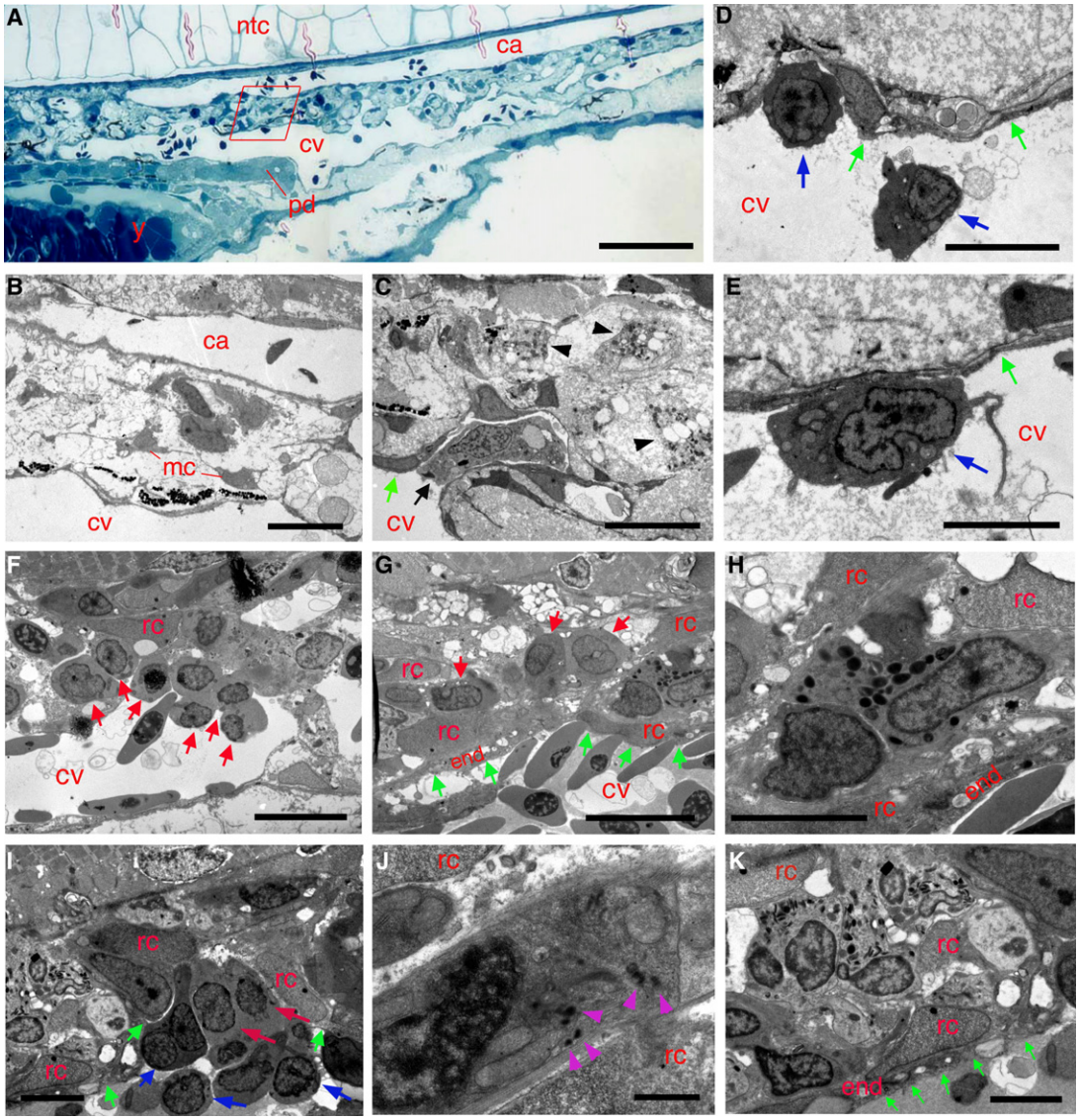

Figure 3. Ultrastructure of the Caudal Hematopoietic Tissue

(A–E) 2 dpf.

(A) Light microscopy view of a longitudinal section through the CA and CV plexus (rostral left), close to the cloaca (end of pronephric duct (pd)); y, yolk sac.

(B) EM view of area boxed in (A), showing mesenchymal cells (mc) in the space between CA and CV.

(C) Macrophage in CV plexus lumen (arrow) and differentiated macrophages in the mesenchyme (arrowheads).

(D and E) Early, lymphocyte-like hematopoietic precursors in the CV lumen.

(F–K) 5 dpf.

(F and G) Early presumptive myeloid/erythroid progenitors (red arrows) in the CV lumen (F) and in abluminal cell cords (G) within the meshwork of fibroblastic reticular cells (FRCs) (rc).

(H–K) Granulopoiesis in abluminal mesenchyme; (H) eosinophil; (I) myeloblasts (red arrows) and an early precursor (blue arrow); (J) early neutrophilic myelocyte, containing a few, electron-dense cytoplasmic granules (arrowheads); (K) mature neutrophils between FRCs (rc). Note the intimate association between supporting FRCs (rc) and CV endothelium ("end," and green arrows).

Scale bars represent 100 μm in (A); 10 μm in (B), (C), (F), and (G); 5 μm in (D), (E), (H), (I), and (K); and 1 μm in (J).

The Caudal Hematopoietic Tissue Displays a Histological Organization Similar to the Definitive Hematopoietic Tissue of the Pronephros

We then investigated in more detail the histological organization and cell content of the caudal hematopoietic tissue by electron microscopy. At 2 dpf, the mesenchyme around the CV plexus appeared as a loose connective tissue, mainly consisting of irregular mesenchymal cells and macrophages filled with numerous electron-dense cytoplasmic granules and engulfed cell debris (Figures 3A–3C). In the lumen of the CV plexus, we found phagocytic macrophages, sometimes possibly migrating into the connective tissue to differentiate into mature, fixed macrophages (Figure 3C), and also hematopoietic precursors, often associated with the venous endothelium (Figures 3D and 3E). These cells resembled small or

medium lymphocytes, appeared more undifferentiated than myeloblasts, and could correspond to multipotent blood cell precursors.

At 3, 4, and 5 dpf, a hematopoietic tissue grew in association with the CV. It consisted in a stroma formed by the venous endothelium and a network of fibroblastic reticular cells (FRCs) that projected into the hematopoietic tissue from the endothelial cells, with which they were intimately associated (Figures 3F–3K). This stroma contained developing hematopoietic cells, largely myeloblasts, myelocytes, and mature neutrophils, as well as eosinophils (Figures 3G–3K). Overall, the histological organization was remarkably similar to that observed previously in the zebrafish hematopoietic pronephros at slightly later stages (Willett et al., 1999), as well as in the kidney of various adult teleost fishes (Zapata, 1981). We propose to name this tissue the caudal hematopoietic tissue (CHT).

In the CV lumen, groups of early hematopoietic precursors consisting of medium or small lymphocyte-like (candidate multipotent) cells similar to those seen at 2 dpf (Figure 3I and Figures S4A and S4B, blue arrows) and a mixture of presumptive early proerythroblasts and myeloblasts (Figures 3F and 3I and Figure S4B, red arrows) appeared to accumulate on the CV endothelium. Some seem to be crossing through the endothelial cells (Figure 3I and Figure S4A). Both types of precursors were also found in the abluminal compartment (Figure 3G, red arrows, and Figure S4C, blue arrow).

Although thrombocytes could be identified ultrastructurally in the blood by this stage (Figure S4B, inset), it was not possible to document their differentiation in the CHT, because the morphology of thrombocyte precursors in fishes is not known. At 7 dpf, the identified hematopoietic area was smaller than at 5 dpf, but the histological organization and cell content were similar (Figure S4C). At 14 dpf, granulopoiesis was still ongoing in the mesenchyme abluminal and dorsal to the CV (Figures S4E and S4F). The CV lumen still harbored hematopoietic progenitors, but these were now distinct proerythroblasts and erythroblasts, often adherent to the dorsal CV wall and sometimes dividing, in addition to some granulocytes (Figures S4D and S4E).

Thus, ultrastructural analysis confirmed that the CHT is a site of larval hematopoiesis.

The CHT Provides Precursors that Colonize the Thymus and Kidney

What is the nature and fate of the early blood progenitors present in the CHT from 2 dpf? To address this issue, we used an in vivo photoactivatable cell tracer, caged fluorescein-dextran (Gritsman et al., 2000). We injected the caged (nonfluorescent) tracer into 1- to 4-cell embryos. 2–3 days later, we uncaged the fluorescein in the cells of interest with UV light, let the embryos develop until 5 dpf, and processed them for anti-(uncaged) fluorescein immunohistochemistry (Gritsman et al., 2000). We first targeted a 4-somite wide area at the beginning of the tail, at 50 hpf. After fixation of the larvae at 5 dpf, a striking bilateral labeling was observed in the thymus (which in teleost fishes, remains a pair of thymi, situated under the skin ventral to the otic vesicles). The extent of the labeling was such that it delineated the entire thymus (Figures 4A–4C). Uncaging the tracer in more caudal portions of the CHT led to similar labeling of the thymus at 5 dpf (data not shown but see Figures 4E and 4F). In contrast, uncaging the tracer in primitive macrophages in the yolk sac never led to any labeling of the thymus but to dispersed labeled cells in locations consistent with the known tissue distribution of these cells (Figure S5C; Herbomel et al., 2001). Thus by 2 dpf, the whole CHT contained precursors that will colonize the thymus within the next 3 days of development.

In addition to cells in the thymus itself, we frequently found fluorescein-positive cells along a distinct path extending from the thymus to farther caudally, just under the skin (Figures 4C, 4D, and 4F, arrowheads). Interestingly, a similar path of labeled cells could often be seen in embryos in situ hybridized for *c-myb* or *ikaros* mRNA (Figures 4I and 4J; see also Figures S3B and S3C), and not in ISHs for the (pro)-T cell markers *rag1* or *lck* (Figure 4K), which, unlike the first two, were not expressed in the trunk and tail but only in the thymus.

Outside the thymus area, single labeled cells were found dispersed in various epidermal and subepidermal sites throughout the embryo (Figures 4A and 4E, green arrowheads). Close examination revealed histological locations and cell shapes typical of neutrophils at this stage of development (Figure S5A; data not shown). These cells likely arose from the granulopoiesis observed in the CHT.

When we uncaged the tracer in the CHT at 3 dpf, 2 days later we found a similar labeling of numerous cells in the thymus and single amoeboid leukocytes in the tissues (Figures 4E and 4F and Figure S5A, panels g and h). But in contrast with the uncaging at 2 dpf, labeled cells were also found in the kidney, around and caudal to the pronephric glomerulus (Figures 4E and 4G).

These results demonstrate that the CHT contains precursors responsible for the early seeding of the definitive hematopoietic organs, thymus and kidney, as previously suggested by our in situ hybridization data. Immigrants to the thymus are present in the tail already at 2 dpf, whereas those that will seed the kidney are present in the tail by 3 dpf, but not yet at 2 dpf.

The CHT Is Seeded by Precursors Present in the Zebrafish AGM

Since the expression of *c-myb*, *runx1*, and *ikaros* progressively shifts—between 2 and 3 dpf—from the DA-PCV joint (hereafter referred to as "DP joint") in the trunk to the CHT, it was tempting to hypothesize that the myb$^+$ precursors first found in the trunk DP joint may seed the hematopoietic stroma of the CHT, then expand and differentiate there, just like HSCs born in the AGM of the mouse embryo seed the fetal liver, where fetal hematopoiesis takes place.

To test this hypothesis, we laser-uncaged fluorescein-dextran precisely in the DP joint at 2 dpf (Figures 5A and 5B). When the cell fates were analyzed at 5 dpf, a heavy, bilateral labeling of the thymus and of the kidney "marrow" was obtained (Figures 5C–5F), as well as labeling of single, dispersed amoeboid leukocytes (Figure S5A, panels i–k), as previously obtained when uncaging the CHT at 3 dpf. At higher magnification, the labeled cells in the thymus appeared interspersed among unlabeled cells of similar morphology, that of the thymocytes, which represent more than 90% of the thymus cell

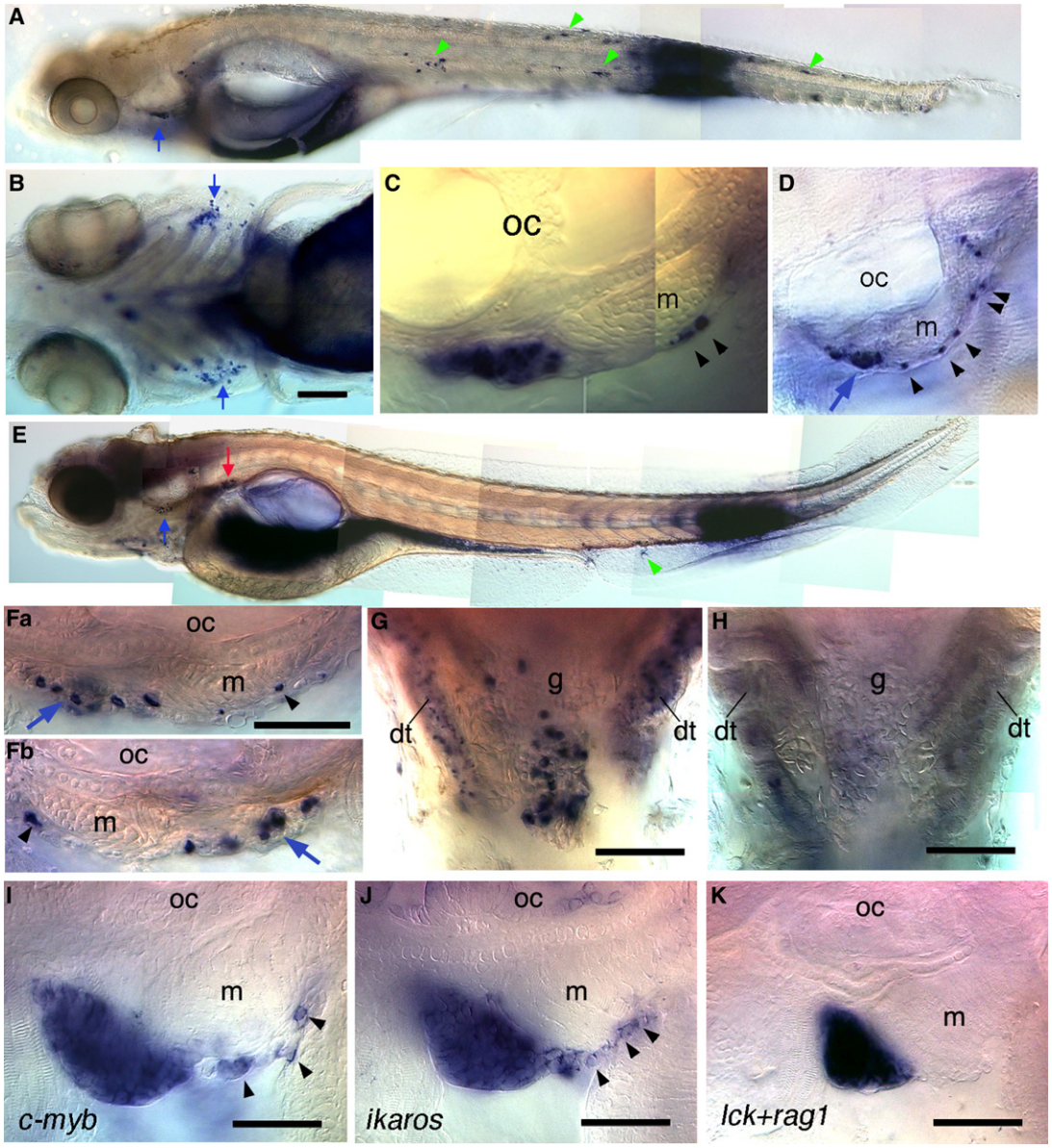

Figure 4. The Tail Contains Future Immigrants to the Thymus and Pronephros

(A–C) Caged fluorescein-dextran-injected embryo exposed to UV light in the tail at 48 hpf, fixed and immunostained for fluorescein at 5 dpf.

(A) Apart from the large dark spot at the site of uncaging, and the dark gut and yolk (see Experimental Procedures), all spots are labeled cells that emigrated from the initial site of uncaging: to the thymus in large number (arrow), and to various sites as single cells, green arrowheads pointing at those shown in detail in Figure S4 (same in [E]).

(B) Ventral view, showing labeling of both thymi (arrows).

(C and D) Lateral view of the labeled left thymus (C), and of that of another embryo treated in the same way (D), showing a subepidermal path of labeled cells (arrowheads) to the thymus (arrow).

(E–G) Embryo in which fluorescein was laser-uncaged throughout a portion of the caudal hematopoietic tissue at 72 hpf, followed by immunostaining at 5 dpf. The labeled thymi (blue arrows) and pronephros (red arrow) are shown at higher magnification in (F) and (G), respectively; (F) left (Fa) and right (Fb) lateral views; (G) ventral view rostral up.

(H) Similar ventral view of a control embryo (caged fluorescein-dextran-injected but not uncaged); in (G), beside the genuinely labeled cells around and above the glomerulus (g), the distal pronephric tubules (dt) show a vesicular labeling (see Experimental Procedures).

(I–K) In situ hybridization for (I) *c-myb* at 5 dpf, (J) *ikaros* at 6 dpf; (K) *lck+rag1* at 5 dpf reveals a path of cells caudal to the thymus for *c-myb* and *ikaros* (arrowheads), but not for *lck+rag1*.

m, muscle. Scale bars represent 100 μm in (B) and 50 μm in (F)–(K).

content at this stage (Willett et al., 1999): small round cells with a mean size of 5.5 μm (Figure 5E), with some amoeboid ones, similar in size to the presumptive HSCs colonizing the kidney (Figures 5F and 5F′) and clearly smaller than the amoeboid myeloid cells dispersed in the tissues (10 μm in length versus 15–20 μm; Figures S5A and S5B). In addition, labeled cells with hematopoietic progenitor morphology were found throughout the CHT (Figure 5G), organized in patterns reminiscent of those seen for *c-myb* expression:

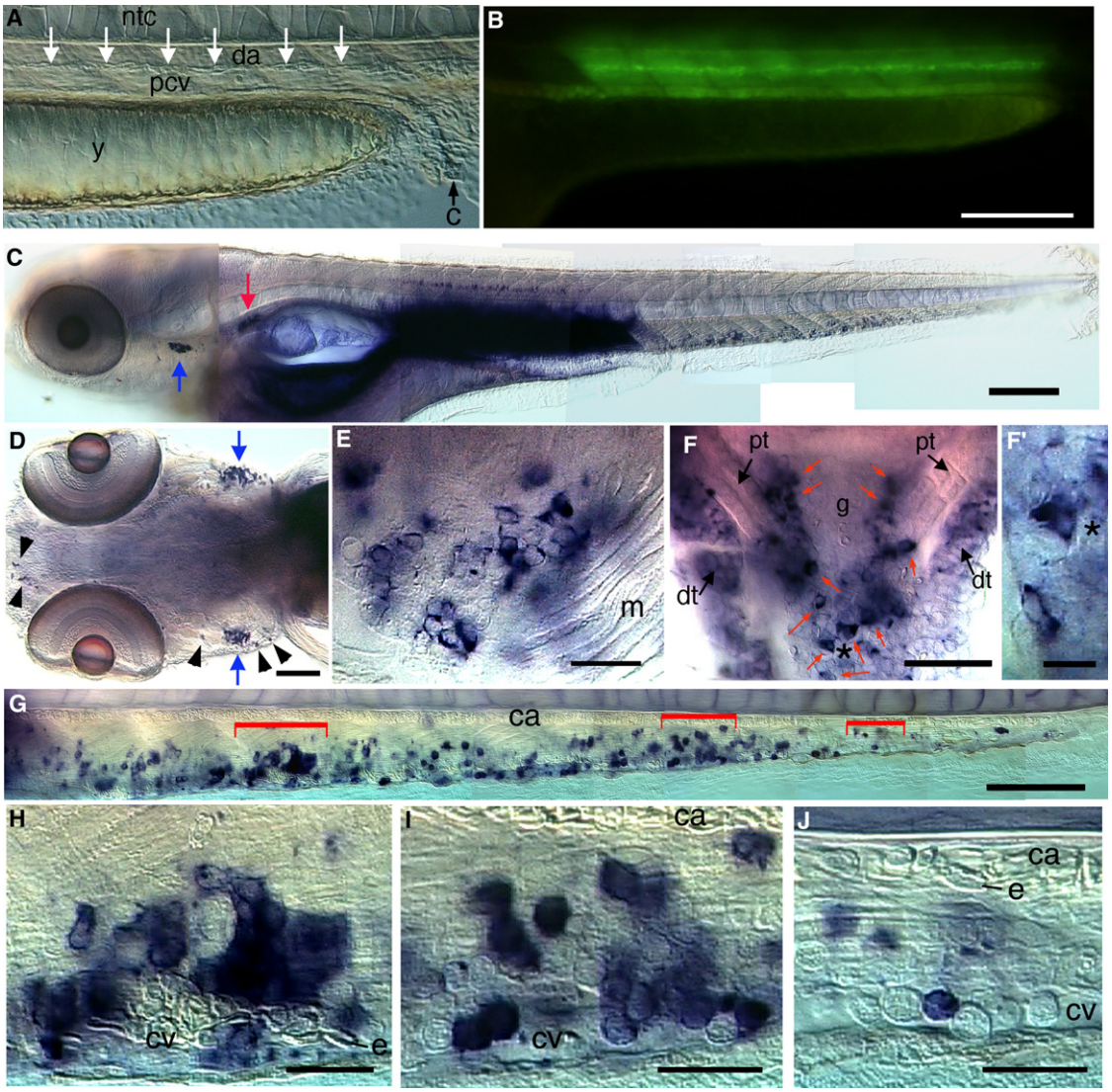

Figure 5. The Trunk DA-PCV Joint Contains Precursors that Will Seed the Caudal Hematopoietic Tissue, Thymus, and Pronephros

(A) DIC video image of a live 2 dpf embryo at the posterior trunk level, focused on the sagittal plane; arrows point at the DA-PCV joint targeted with the laser in (B).

(B) Fluorescence of fluorescein just laser-uncaged all along the DA-PCV joint. The overlying diffuse labeling is due to marginal uncaging in the somite muscle overlying the target followed by diffusion within the somite muscle fibers.

(C–J) Anti-fluorescein immunostaining performed 3 days later (5 dpf).

(D) Ventral view of the head, showing the two thymi (arrows); arrowheads point at labeled leukocytes outside the thymi.

(E) Magnified ventral view of the right thymus, showing individual labeled thymocytes among unlabeled ones.

(F) Pronephros (ventral view, rostral up), with genuinely labeled cells (red arrows) around the glomerulus (g) and vesicular labeling of distal tubules (dt); two labeled cells (asterisk) are shown magnified in (F′).

(G–J) Caudal hematopoietic tissue, lateral view, rostral left; areas bracketed in (G) are shown magnified in (H)–(J). Note that none of the hundreds of primitive erythrocytes fixed in the CA is labeled.

pt, proximal pronephric tubule; e, erythrocyte. Scale bars represent 200 μm in (C); 100 μm in (D) and (G); 50 μm in (F); 20 μm in (E), (H)–(J); 10 μm in (F′).

interconnected labeled cell clusters intermingled with negative ones, with labeled cells both in the mesenchyme and marginated in the CV lumen (Figures 5G–5J, compare with Figure 2I).

Uncaging various segments of the DP joint at 2 dpf revealed that its entire rostro-caudal extent provides cells that will seed the CHT, thymus, and kidney (data not shown). Finally, uncaging the tracer in the DP joint at 3 dpf rather than 2 dpf led at 5 dpf to a similar amount of cell labeling in the kidney, but to less labeling in the thymus and CHT (Figure S5B).

Altogether, these results demonstrate that the DP joint in the trunk, even though exceedingly narrow by 2 dpf (Figure 5A), gives rise to many of the hematopoietic precursors that accumulate and differentiate in the caudal stroma, then migrate and colonize the definitive lympho-hematopoietic organs. Furthermore, the presence of future immigrants to the kidney in the trunk at 2 and

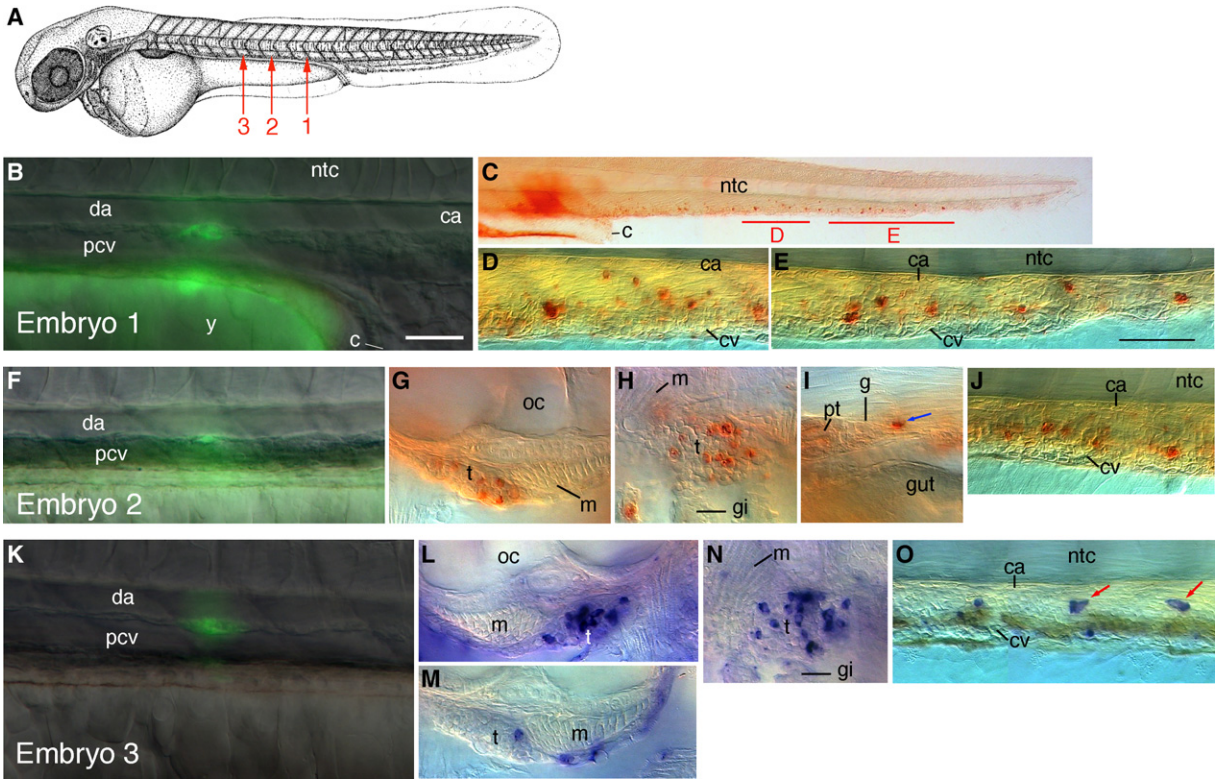

Figure 6. Progeny at 5 dpf of Single or Close-to-Single Cells Labeled in the DP Joint at 2 dpf

In each embryo, at 2 dpf, one single cell that could be discerned by DIC optics between the juxtaposed DA and PCV walls was focused and subjected to a 1 s laser hit. Green fluorescence was recorded immediately and overlayed on the DIC image (B, F, K); one cell was visibly uncaged in embryo 2, and 2–3 cells in embryos 1 and 3. Anti-fluorescein immunostaining was performed at 5 dpf.

(A) Rostro-caudal position of the cell targeted in the DP joint of embryos 1, 2, and 3.

(C–E) In embryo 1, labeled progeny was mostly found in the CHT.

(G–J) Embryo 2 displayed numerous labeled cells in both left (G) and right (H) thymus (arrows), one adjacent to the pronephric glomerulus (I, arrow), and several in the CHT (J).

(L–O) Embryo 3 displayed numerous labeled cells in the right thymus ([L], [N], lateral and ventral views, respectively), only one in the left thymus (M), and several in the CHT (O) including two amoeboid, presumptively myeloid cells (arrows).

In all panels, rostral is to the left, except for those showing the right thymus (H, L, N), in which rostral is to the right. All views are lateral except (H) and (N), which are ventrolateral. To help orientation in the thymus area, the same muscle caudally adjacent to the thymus is indicated in all thymus views by (m). gi, gills; pt, proximal tubule. Scale bars represent 50 μm.

3 dpf, and in the CHT at 3 dpf but not 2 dpf, indicates that the multipotent blood precursors released by the DP joint to the CHT up to 2 dpf and after 2 dpf have distinct fates: the first ones will differentiate along myeloid lineages in the CHT and provide lymphoblasts to the thymus, while only the second wave (released after 2 dpf) will provide immigrants to the kidney—presumably the definitive HSCs.

Dynamics of Cell Seeding and Expansion from AGM to CHT and Thymus

We then followed up directly the fluorescence of the uncaged tracer in individual live embryos at various intervals after laser-uncaging the whole DP joint at 2 dpf. 24 hr later, the CHT already contained numerous fluorescent cells, including presumptive pairs of sister cells (Figure S6A, arrows). After one more day (4 dpf), the number of fluorescent cells in the CHT had expanded, and their mean fluorescence level had decreased, suggesting local proliferation of the labeled cells within the CHT between 3 and 4 dpf (Figure S6B).

In parallel embryos, 1 day after uncaging the DP joint at 2 or 3 dpf, labeled cells could already be immunodetected in the thymus, although less than by 2 or 3 days after uncaging, and not always in both thymi (Figures S6C–S6E).

To better document the expansion of AGM precursors in the subsequent hematopoietic tissues, we refined our cell-tracing analysis by uncaging the tracer in single or close-to-single cells within the DP joint at 2 dpf. Each embryo was subjected to a single laser hit, aimed at one cell that could be discerned by DIC optics between the juxtaposed DA and PCV (Figure 6A). Fluorescence imaging performed immediately thereafter suggested that between 1 and 3 cells had been actually uncaged to some extent (Figures 6B, 6F, and 6K). 6/18 such "single hit" embryos led to an abundant progeny of labeled cells 3 days later, in the CHT and/or in the thymus. Three of them are shown in Figure 6. Most notably, embryo 1 displayed an abundant labeled progeny dispersed throughout the CHT (Figures 6B–6E). Embryo 2, in which only the targeted AGM cell had been visibly uncaged (Figure 6F), showed labeled cells in the CHT, numerous

cells in both thymi, and one cell in the kidney, abutting the pronephric glomerulus (Figures 6G–6J). Embryo 3 (Figures 6K–6O) displayed numerous labeled cells in the right thymus but virtually none in the left thymus, suggesting intrathymic proliferation of 1 or 2 labeled immigrants, and a few cells in the CHT, including two with amoeboid morphology suggesting granulocytic differentiation.

The Seeding of Caudal Hematopoiesis by AGM Precursors Requires Blood Circulation

Because of the small size of zebrafish embryos and larvae, oxygen supply by circulating erythrocytes is entirely dispensable for the first 2 weeks of development (oxygen diffusion from the water is sufficient). We therefore prevented the onset of blood circulation by morpholino-mediated suppression of cardiac tropomyosin, leading to "silent heart" morphants (Sehnert et al., 2002). Apart from cardiac edema, *sih* morphants develop normally until about 2 dpf, and then they show increasing developmental defects, likely resulting from lack of yolk nutriment delivery through the blood and absence of renal function (Serluca et al., 2002). We injected the *sih* morpholino into CD41-gfp and gata1-dsred double transgenic embryos, so as to follow up simultaneously the distribution of noncirculating DsRed$^+$ primitive erythrocytes and the emergence of GFP$^+$ progenitors in individual embryos through time. These GFP$^+$ cells include thrombocytes, thrombopoietin receptor-dependent presumptive prothrombocytes (Lin et al., 2005), as well as earlier hematopoietic progenitors (data not shown).

In *sih* morphants, GFP$^+$ cells did appear, and their number increased from 2 to 3.5 dpf, but they were confined to the trunk instead of the tail (Figure 7). Overall they were, however, less numerous at all stages than in control embryos, suggesting that the CHT microenvironment is more appropriate to the development of hematopoiesis. c-myb$^+$ progenitors also accumulated in the trunk instead of the tail (Figures 7M and 7N). The lack of hematopoietic progenitors in the tail of *sih* morphants was not due to a steric hindrance of their migration from trunk to tail by the mass of noncirculating primitive erythrocytes, since past 2 dpf, the latter were actually found rostral to the bulk of DsRed$^+$ cells in the trunk (Figures 7D–7F, arrows). These results demonstrate that (1) no early hematopoietic precursors are generated in the tail; and (2) even though the hematopoietic precursors present in the posterior DP joint are located close to the caudal stroma, they can seed it only through the circulation.

Discussion

We have here established that in the zebrafish, after primitive hematopoiesis and before the establishment of definitive hematopoiesis in the kidney, an intermediate, larval site of hematopoiesis exists in the tail. We propose to call it the caudal hematopoietic tissue, or CHT. It is initiated around a transient structure, the caudal vein plexus, reaches its peak activity by 5–6 days pf, but remains hematopoietic until at least 2 weeks pf, associated with the definitive caudal vein into which the CV plexus evolved. The CHT supports the accumulation and expansion of AGM-derived blood precursors, and the differentiation of prothrombocytes and granulocytes, both neutrophils and eosinophils. In lower vertebrates, erythrocyte and much of thrombocyte differentiation occur in the vessels (Zapata et al., 1995). The relatively late appearance (10–14 dpf) of identifiable early erythroblasts marginated on the CV wall suggests that early progenitors in the CHT may not engage in the erythroid lineage before several days.

The cytoarchitecture of the CHT is strikingly similar to that of the definitive site of hematopoiesis in the kidney, as well as to hematopoietic stromas of other species, such as the bone marrow of mammals. By 2 dpf, the several branches of the CV plexus form sinusoids in which the blood flow is slowed down, favoring the homing of circulating progenitors. By 3 dpf, in close contact with the sinusoids, a typical network of fibroblastic reticular cells (FRCs) has formed, between which hematopoietic progenitors expand and differentiate. In mammals, non-endothelial stromal cell lines that can support hematopoiesis in vitro probably derive from similar FRCs (Dorshkind, 1990). Where could the FRCs of the zebrafish CHT originate from? By 2 dpf, the CV plexus is surrounded by an enlarged extracellular matrix (ECM) containing sparse, irregular mesenchymal cells, whereas some presumptive HSCs are already homing in and undergoing some differentiation. A day later, the CV plexus and surrounding ECM have undergone a striking retraction, blood has ceased flowing through most of the plexus except the definitive CV, and the network of FRCs has formed. Thus, a possible scenario would be that the mesenchymal cells seen at 2 dpf around the CV plexus generated the enlarged ECM (e.g., through secretion of hyaluronan), which may be required for CV plexus formation; then, these mesenchymal cells differentiated into FRCs, with consequent tissue retraction. The steady process of rostrocaudal extension of the tail may also contribute to the dorsoventral retraction of the CV plexus. Remarkably, it is this retraction that soon brings the definitive CV into contact with the hematopoietic cells derived from the precursors that homed through the more dorsal branches of the plexus, thereby facilitating their entry and gathering into the definitive CV lumen over the next days.

The CV plexus likely is a very efficient "trap" for circulating hematopoietic progenitors, or even leukocytes in general. This is strikingly illustrated by two so far unexplained observations from the literature: when GFP$^+$ whole kidney marrow leukocytes from adult β-actin-gfp transgenic zebrafish (Traver et al., 2003) or GFP$^+$ thymocytes from adult lck-gfp transgenics (Langenau et al., 2004) were injected into the sinus venosus of 2 dpf embryos, they were found in the thymus 2–3 days later, but also massively, already after 1 day, in the ventral tail—actually in the CHT. It is clear from our data that 2 dpf should be the optimal stage to accommodate the homing of these transplanted cells in the CHT: the CV plexus is fully functional and surrounded by a still largely empty mesenchymal space.

Our WISH and cell-tracing data show that in the normal fish larva, most if not all blood precursors that seed the definitive hematopoietic organs, thymus and kidney, first accumulate in the CHT (including its patchy extension in the trunk along the PCV from 4 dpf). Among the early hematopoietic markers expressed in the CHT,

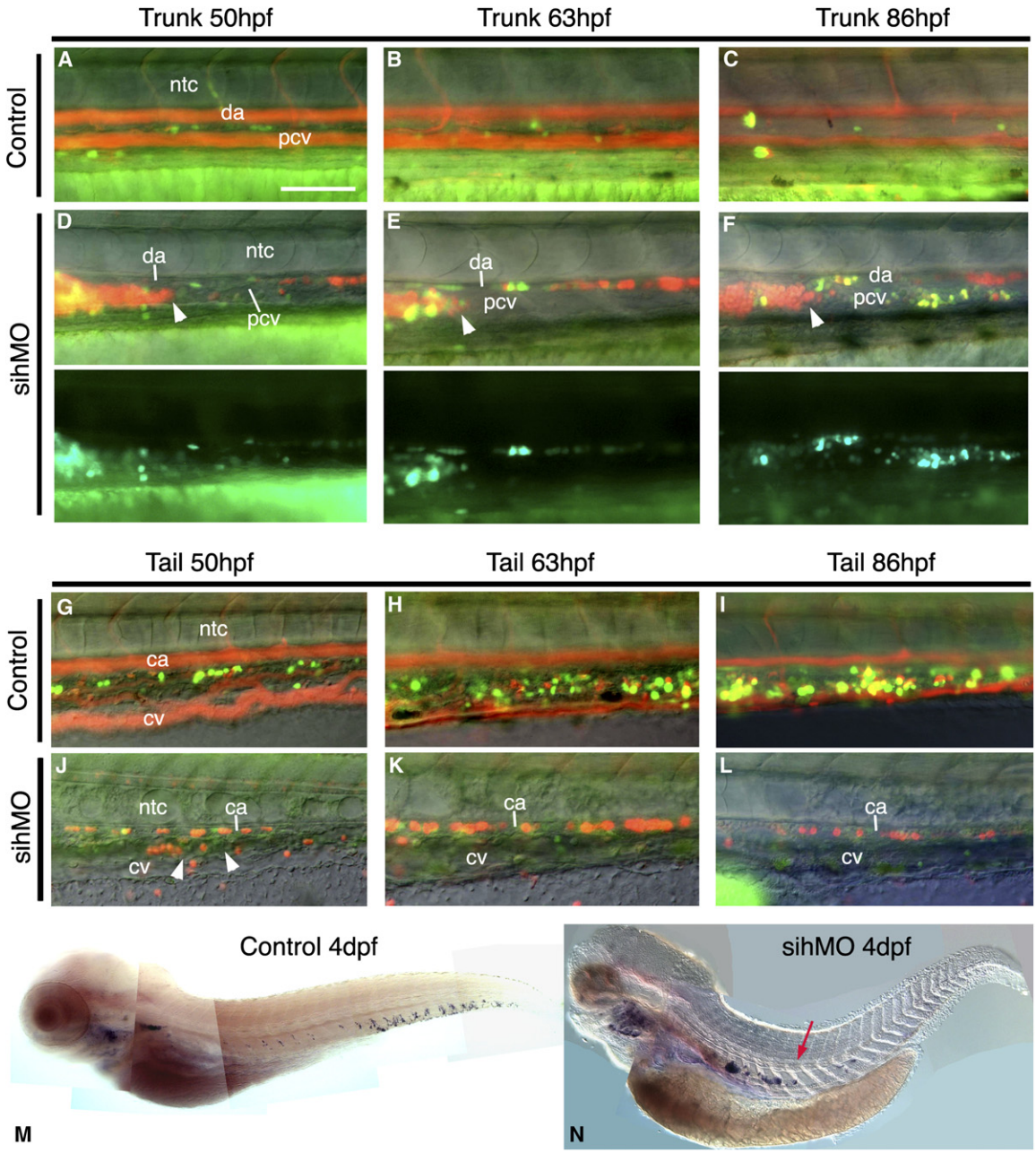

Figure 7. The Seeding of Caudal Hematopoiesis Requires Blood Circulation

(A–L) Real-time follow-up of representative control and *silent heart* morphant [CD41-gfp; gata1-dsred] embryo, at the trunk (A–F) and tail (G–L) level; green+red fluorescence overlaid on DIC images (lateral views, rostral left). In the control embryo, the flow of circulating DsRed$^+$ primitive erythrocytes delineates blood circulation; GFP$^+$ cells develops in the tail (G–I), barely in the trunk (A–C). In the *silent heart* morphant, many of the noncirculating primitive erythroblasts are gathered in a big mass in the rostral trunk (an arrowhead indicates its caudal border) (D–F); GFP$^+$ cells develop in the trunk ([D]–[F], lower panels show green channel alone) and not in the tail (J–L), despite the presence of a normal CV plexus at 2 dpf ([J], arrowheads). Scale bar represents 100 μm.

(M and N) In situ hybridization for *c-myb* in control and *sih* morphant embryos.

we found that the recent immigrants to the thymus are c-myb$^+$, ikaros$^+$, runx$^-$, scl$^-$. The thymus is labeled homogeneously by *c-myb* and *ikaros* expression since the very beginning of its known colonization (72 hpf), so these two markers are doubtlessly coexpressed by all thymic immigrants. Furthermore, as expected from markers of immigrating cells, in situ hybridization for these two genes also reveals some labeled cells in the vicinity of the thymus, notably along a path running just beneath the epidermis caudal to the thymus, that also appears in our in vivo cell tracing data. In contrast, we found no runx1$^+$, scl$^+$, or rag1$^+$ cells in the vicinity of the thymus, indicating that: (1) *runx1* and *scl* must have become extinguished before the immigrants reached the thymus—presumably while they were still in the CHT; and (2) *rag1* is activated in these cells only once

they have settled in the thymus. We found that the immigrants to the kidney, the site of definitive, multilineage hematopoiesis, express the same markers as found for the thymic immigrants plus *scl* and *runx1*—the two hematopoietic factors in the series assessed here that are considered the most early acting. This suggests that the immigrants to the kidney are multipotent HSCs, while those immigrating to the thymus may already have a more restricted hematopoietic potential, i.e., become already lymphoid committed in the CHT.

Our in vivo cell tracing experiments demonstrate that the CHT, thymus, and kidney are seeded by precursors born in the trunk, precisely in the small space between the closely juxtaposed DA and PCV where *runx1* and *c-myb* are expressed between 1 and 3 dpf. These results validate experimentally for the first time the functional homology of this site with the "AGM" of amniote embryos. The cord of c-myb$^+$ precursors begins rostrally at somite 6, precisely where the rostrally bilateral PCVs become one axial vessel juxtaposed to the DA (data not shown). Therefore, to reflect its symmetrical situation relative to the DA and PCV, we prefer to name this site of HSC generation the "DA-PCV joint" or "DP joint" (rather than the previously used "ventral wall of the DA" or "DA-associated cells") or the zebrafish AGM when referring to its functional significance.

The sequence of developmental hematopoiesis revealed by our data in the zebrafish is strikingly similar to that found in the mouse, considering the relative timing of AGM activity, first hematopoietic differentiation in the intermediate site (fetal liver versus CHT), first colonization of the thymus, peak number of HSCs in the fetal or larval site, and first detected hematopoiesis in the final organ (bone marrow versus kidney) (Figure S7).

Our cell-tracing data in the fish reveal that the precursors released by the DP joint to the CHT until 2 dpf and past 2 dpf have distinct fates, only the latter ultimately providing immigrants to the kidney—presumably the definitive HSCs. This finding, together with all data presented above, suggests two possible models. In model 1, the DP joint successively releases two different types of precursors. As definitive HSCs are generated in the DP joint, they undergo rounds of asymmetric cell divisions there, through which they produce non-HSC but still multipotent progenitors (MPPs) that enter the circulation and home in the still immature CHT discussed above. In the CHT, these MPPs provide progenitors for the myeloid and thrombocytic lineages, and (likely lymphoid-committed) immigrants to the thymus. At some time between 2 and 3 dpf, the definitive HSCs themselves start to leave the DP joint and home to the CHT. There, they expand, possibly produce more MPPs (for the CHT keeps providing immigrants to the thymus), and start being recruited by the kidney by 4 dpf.

In model 2, precursors released by the DP joint at any time are all equivalent, potential HSCs. The first ones that home in the tail, up to 2 dpf, find there a still immature CHT (no FRC network yet), in which they can rapidly differentiate, into myeloid and lymphoid-committed progenitors, but not expand as HSCs. In contrast, those arriving after 2 dpf find a mature hematopoietic stroma (with a structured FRC network) that can support their expansion and maturation as HSCs. Presently we tend to favor the latter model, for it integrates the rapid change in CHT structure that parallels the change in precursor fate.

In any case, the notion of a differential fate of HSCs according to their release date from the AGM may apply also to the seeding by mouse AGM cells of the fetal liver and bone marrow, for in fetal liver as in the zebrafish CHT, hematopoietic differentiation precedes expansion of the HSC pool.

The data presented here fill gaps in our knowledge of developmental hematopoiesis in the zebrafish. They evidence close parallels between species at opposite ends of the vertebrate phylum. They demonstrate a direct lineage relationship between AGM cells and the seeders of the successive hematopoietic organs. Finally, they contribute to delineating the distinct phenotype of the early immigrants to the thymus, a highly debated matter in mammals.

Experimental Procedures

Zebrafish Stocks and Embryo Treatments

Wild-type AB and transgenic stocks of zebrafish were maintained as described (Westerfield, 2000). The fli1-gfp, gata1-dsred, and CD41-gfp transgenic lines have been described (Lawson and Weinstein, 2002; Traver et al., 2003; Lin et al., 2005). Embryos were grown in presence of 0.003% 1-phenyl-2-thiourea to prevent melanin pigmentation (Westerfield, 2000) and staged according to Kimmel et al. (1995). The *silent heart* morpholino sequence and dose injected in 1- to 4-cell stage embryos were as described by Sehnert et al. (2002). The resulting lack of heartbeat was checked throughout the experiments.

Whole-Mount RNA In Situ Hybridization

Whole-mount RNA in situ hybridization (WISH) was performed according to Thisse (http://zfin.org/zf_info/zfbook/chapt9/9.82.html) following the high stringency option (hybridization in 65% formamide), on embryos fixed at 26 hpf, 35 hpf, 2, 3, 4, 5, 6, and 7 dpf.

Cell Tracing through Uncaging of Caged-Fluorescein Dextran

Embryos were injected at the 1- to 4-cell stage with 1 nl of a 1:3 mix of fixable and nonfixable caged fluorescein-dextran 10,000 (Molecular Probes) together with 1/10 v/v rhodamine-dextran 10,000 (all from 5 mg/ml stock solutions in 120 mM KCl), and then allowed to develop in the dark, except for their manipulation, during which illumination was kept minimal. Only embryos displaying homogeneous rhodamine fluorescence were used for uncaging experiments. UV light-mediated fluorescein uncaging was performed through the epifluorescence port of a Nikon 90i microscope, with either the 100W mercury lamp (diaphragm closed, 5 s illumination) or a Micropoint pulsed nitrogen laser (Photonic Instruments), and a 40× dry objective. At 5 dpf, the embryos were fixed with 4% methanol-free formaldehyde (Polysciences) in PBS for 1 hr at room temperature, rinsed in PBS-Tween 0.1%, permeabilized by acetone, and then treated with collagenase as described by Svoboda et al. (2001). They were heat treated at 65°C for 15 min (if later revealed with alkaline phosphatase), then blocked for 2 hr in 10% sheep serum/PBSDT (PBS, 1% DMSO, 0.1% Triton) at room temperature, incubated overnight with anti-fluorescein Fab fragments (Roche) coupled to either alkaline phosphatase (1:4000) or horseradish peroxidase (1:500) at 4°C under gentle agitation, washed with PBSDT at least 6 hr at room temperature, and processed for NBT/BCIP-based revelation of alkaline phophatase activity as in WISH (see above) or for AEC-based revelation of peroxidase activity (Svoboda et al., 2001). Under these conditions, staining unrelated to the cell tracing is restricted to specific structures: (1) in control embryos (injected with caged-fluorescein dextran, but not submitted to UV-mediated uncaging), only the gut (and occasionally the yolk) shows anti-fluorescein immunoreactivity (Figure S5D); and (2) in UV-photoactivated embryos, the pronephric distal tubules (Figures 4G, 4H, and 5F), and some veins show a vesicular staining reflecting their cleaning/recycling activity on blood molecules (that can be visualized with standard fluorescent

dextrans), acting on any trace amount of free uncaged fluorescein-dextran in the blood.

Light and Electron Microscopy

Embryos were anesthetized with 160 μg/ml tricaine and placed in depression slides. Video-enhanced DIC microscopy was performed and recorded as described (Herbomel et al., 1999; Herbomel and Levraud, 2005). Fixed, in situ hybridized or immunostained embryos were imaged with the same tools; for ventral views of the kidney, the intestinal bulb, yolk sac remnant, and swimbladder were removed. Fluorescence images were captured with a Nikon DS5c camera; green, red, and DIC channels were overlaid with the Eclipse software.

For electron microscopy, fish larvae at 2, 4, 5, 7, and 14 dpf (at least four fish for each developmental stage) were fixed and processed as previously described (Willett et al., 1999).

Supplemental Data

Supplemental Data include seven figures and four movies and can be found with this article online at http://www.immunity.com/cgi/content/full/25/6/963/DC1/.

Acknowledgments

We thank L. Zon for the gata1-dsred transgenic zebrafish line and I. Godin, A. Cumano, E. Hirsinger, and M. Redd for their critical reading of the manuscript. This work was supported by an Avenir grant from Inserm and an internal grant from the "Stem cells" horizontal program of the Pasteur Institute. E. Murayama was initially supported by Inserm-Avenir; E. Murayama and K.K. were supported by the European Commission through the FP6 Integrated Project "ZF-Models."

Received: June 6, 2006
Revised: September 19, 2006
Accepted: October 17, 2006
Published online: December 7, 2006

References

Burns, C.E., Traver, D., Mayhall, E., Shepard, J.L., and Zon, L.I. (2005). Hematopoietic stem cell fate is established by the Notch-Runx pathway. Genes Dev. *19*, 2331–2342.

Davidson, A.J., and Zon, L.I. (2004). The 'definitive' (and 'primitive') guide to zebrafish hematopoiesis. Oncogene *23*, 7233–7246.

Dorshkind, K. (1990). Regulation of hemopoiesis by bone marrow stromal cells and their products. Annu. Rev. Immunol. *8*, 111–137.

Gering, M., and Patient, R. (2005). Hedgehog signaling is required for adult blood stem cell formation in zebrafish embryos. Dev. Cell *8*, 389–400.

Godin, I., and Cumano, A. (2002). The hare and the tortoise: an embryonic haematopoietic race. Nat. Rev. Immunol. *2*, 593–604.

Gritsman, K., Talbot, W.S., and Schier, A.F. (2000). Nodal signaling patterns the organizer. Development *127*, 921–932.

Herbomel, P., and Levraud, J.P. (2005). Imaging early macrophage differentiation, migration, and behaviors in live zebrafish embryos. Methods Mol. Med. *105*, 199–214.

Herbomel, P., Thisse, B., and Thisse, C. (1999). Ontogeny and behaviour of early macrophages in the zebrafish embryo. Development *126*, 3735–3745.

Herbomel, P., Thisse, B., and Thisse, C. (2001). Zebrafish early macrophages colonize cephalic mesenchyme and developing brain, retina, and epidermis through a M-CSF receptor-dependent invasive process. Dev. Biol. *238*, 274–288.

Isogai, S., Horiguchi, M., and Weinstein, B.M. (2001). The vascular anatomy of the developing zebrafish: an atlas of embryonic and early larval development. Dev. Biol. *230*, 278–301.

Kimmel, C.B., Ballard, W.W., Kimmel, S.R., Ullmann, B., and Schilling, T.F. (1995). Stages of embryonic development of the zebrafish. Dev. Dyn. *203*, 253–310.

Langenau, D.M., Ferrando, A.A., Traver, D., Kutok, J.L., Hezel, J.P., Kanki, J.P., Zon, L.I., Look, A.T., and Trede, N.S. (2004). In vivo tracking of T cell development, ablation, and engraftment in transgenic zebrafish. Proc. Natl. Acad. Sci. USA *101*, 7369–7374.

Lawson, N.D., and Weinstein, B.M. (2002). In vivo imaging of embryonic vascular development using transgenic zebrafish. Dev. Biol. *248*, 307–318.

Liao, E.C., Paw, B.H., Oates, A.C., Pratt, S.J., Postlethwait, J.H., and Zon, L.I. (1998). SCL/Tal-1 transcription factor acts downstream of cloche to specify hematopoietic and vascular progenitors in zebrafish. Genes Dev. *12*, 621–626.

Lieschke, G.J., Oates, A.C., Crowhurst, M.O., Ward, A.C., and Layton, J.E. (2001). Morphologic and functional characterization of granulocytes and macrophages in embryonic and adult zebrafish. Blood *98*, 3087–3096.

Lin, H.F., Traver, D., Zhu, H., Dooley, K., Paw, B.H., Zon, L.I., and Handin, R.I. (2005). Analysis of thrombocyte development in CD41-GFP transgenic zebrafish. Blood *106*, 3803–3810.

Sehnert, A.J., Huq, A., Weinstein, B.M., Walker, C., Fishman, M., and Stainier, D.Y. (2002). Cardiac troponin T is essential in sarcomere assembly and cardiac contractility. Nat. Genet. *31*, 106–110.

Serluca, F.C., Drummond, I.A., and Fishman, M.C. (2002). Endothelial signaling in kidney morphogenesis: a role for hemodynamic forces. Curr. Biol. *12*, 492–497.

Svoboda, K.R., Linares, A.E., and Ribera, A.B. (2001). Activity regulates programmed cell death of zebrafish Rohon-Beard neurons. Development *128*, 3511–3520.

Thompson, M.A., Ransom, D.G., Pratt, S.J., MacLennan, H., Kieran, M.W., Detrich, H.W., 3rd, Vail, B., Huber, T.L., Paw, B., Brownlie, A.J., et al. (1998). The cloche and spadetail genes differentially affect hematopoiesis and vasculogenesis. Dev. Biol. *197*, 248–269.

Traver, D., Paw, B.H., Poss, K.D., Penberthy, W.T., Lin, S., and Zon, L.I. (2003). Transplantation and in vivo imaging of multilineage engraftment in zebrafish bloodless mutants. Nat. Immunol. *4*, 1238–1246.

Westerfield, M. (2000). The Zebrafish Book. A Guide for the Laboratory Use of Zebrafish (*Danio rerio*) (Eugene, OR: University of Oregon).

Willett, C.E., Cortes, A., Zuasti, A., and Zapata, A.G. (1999). Early hematopoiesis and developing lymphoid organs in the zebrafish. Dev. Dyn. *214*, 323–336.

Zapata, A. (1981). Lymphoid organs of teleost fist. II. Ultrastructure of renal lymphoid tissue of *Rutilus rutilus* and *Gobio gobio*. Dev. Comp. Immunol. *5*, 685–690.

Zapata, A.G., Torroba, M., Vicente, A., Varas, A., Sacedon, R., and Jimenez, E. (1995). The relevance of cell microenvironments for the appearance of lympho-haemopoietic tissues in primitive vertebrates. Histol. Histopathol. *10*, 761–778.